Nuclear Mathematical and Computational Sciences: A Century in Review, A Century Anew
Gatlinburg, Tennessee, April 6-11, 2003, on CD-ROM, American Nuclear Society, LaGrange Park, IL (2003)

FORMS OF APPROXIMATE RADIATION TRANSPORT

Thomas A. Brunner
Sandia National Laboratories
PO Box 5800
Albuquerque, NM 87185-1186
tabrunn@sandia.gov

ABSTRACT

Photon radiation transport is described by the Boltzmann equation. Because this equation is difficult to solve, many different approximate forms have been implemented in computer codes. In particular, the diffusion approximation, discrete ordinates approximation, the spherical harmonics approximation, and the Monte Carlo method are reviewed. Three test problems illustrate the characteristics of each of the approximations.

Key Words: Boltzmann transport equation, test problems

1. INTRODUCTION

The Boltzmann transport equation describes how a variety of different types of particles travel through a material. It is generally considered the most accurate description of the statistical average density of particles in a system. The Boltzmann equation is very general, and every discipline has a different way to write it that fits their needs best. Here, the intensity $I(\mathbf{r}, \mathbf{\Omega}, \varepsilon, t) = h\nu f$ is the primary variable, where $f(\mathbf{x}, \mathbf{\Omega}, \varepsilon, t)$ is a phase space density, ν is the photon frequency with energy $\varepsilon = h\nu$, and h is Planck's constant. The energy integrated Boltzmann equation for radiation transport is [1, 14, 17, 21]

$$\frac{1}{c}\frac{\partial I}{\partial t} + \mathbf{\Omega}\cdot\nabla I = -\sigma_t I + \frac{\sigma_s}{4\pi}\int_{4\pi} I \ \mathrm{d}\mathbf{\Omega}' + \sigma_a \frac{1}{4\pi}B(T_m) + S. \tag{1}$$

In addition to Eq. 1, which describes the evolution of the energy density of the photons, there is another equation that describes the energy content of the material. This equation is

$$\frac{\partial \rho C_v T_m}{\partial t} = -\int_{4\pi} c\sigma_a \left(\frac{1}{4\pi}B(T_m) - I\right) \ \mathrm{d}\mathbf{\Omega} + Q_m. \tag{2}$$

In Eq. 1 and Eq. 2, c is the speed of light, $\mathbf{\Omega}$ is the unit angle vector, ρ is the material density, C_v is the specific heat, T_m is the material temperature, $\sigma_t = \sigma_s + \sigma_a$ are the total, scattering, and absorption opacities with units of inverse length, S is an external source of photon energy, Q_m is an external source of material heating, and $B(T_m)$ is the black body function

$$B(T_m) = \frac{8\pi^5 k^4}{15h^3c^3}T_m^4 = aT_m^4, \tag{3}$$

where a is the black body constant, and k is Boltzmann's constant.

Not only is Eq. 1 difficult to solve, but the intensity I contains much more detailed information than is frequently needed to solve a particular problem. In fact, the coupling with the material in Eq. 2 is only

through the radiation energy density, which is the integral of I over all angles, or

$$E = \int_{4\pi} I \, \mathrm{d}\mathbf{\Omega} \,, \tag{4}$$

where E is radiation energy density.

Eq. 1 is difficult to solve directly, and approximation is nearly always made before solving it. Several of the most popular approximations used in the radiation transport community are reviewed here, namely the diffusion approximation, the discrete ordinates approximation, the spherical harmonics approximation, and the Monte Carlo method.

2. THE APPROXIMATIONS

The common approaches to solving Eq. 1 are to use the diffusion approximation [2, 5, 6, 12, 13, 15, 19, 20, 23], the discrete ordinates approximation [1, 16, 18, 21], the spherical harmonics approximation [3, 4, 7, 22], and the Implicit Monte Carlo method [9, 10]. The diffusion approximation has some serious defects, and many enhancements that have extended its range of applicability are in use. Only the Boltzmann equation, Eq. 1, is being approximated in all these methods; the material energy equation, Eq. 2, is unchanged.

2.1. Diffusion

In the diffusion approximation the intensity I is assumed to have the form

$$I(\mathbf{r}, \mathbf{\Omega}, t) = \frac{1}{4\pi} E + \frac{3}{4\pi} \mathbf{\Omega} \cdot \mathbf{F}, \tag{5}$$

where $\mathbf{F}$ is the radiative flux defined by

$$\mathbf{F} = \int_{4\pi} \mathbf{\Omega} I \, \mathrm{d}\mathbf{\Omega} \approx -\frac{1}{3\sigma_t} \nabla E. \tag{6}$$

Eq. 5 and Eq. 6 leads to the diffusion equation, namely

$$\frac{1}{c} \frac{\partial E}{\partial t} - \nabla \cdot \frac{1}{3\sigma_t} \nabla E = \sigma_a \left(4\pi B(T_m) - E\right) + S_E. \tag{7}$$

The diffusion equation is very easy to solve but is inaccurate in optically thin regions and where the gradient of the energy density is large. Flux limited diffusion is an improvement to fix these deficiencies at the cost of making the equations nonlinear. In flux limited diffusion, the equations are modified such that the factor of $1/3$ in Eq. 6 and Eq. 7 is replaced with a nonlinear function of E. For several flux limiters, this nonlinear function is chosen to get the exact transport solution for a particular problem [15, 19].

There has been a fundamental change in the form of the equations; the transport equation (Eq. 1) is hyperbolic, implying that particles (and energy) travels at finite speeds. The time dependent diffusion equation is parabolic, allowing the particles to travel at infinite speed; a small change in one part of the problem immediately affects every other part of the problem.

2.2. Discrete Ordinates

The discrete ordinates approximation assumes that particles can only travel along a few particular directions, instead of the infinite number of directions allowed in Eq. 1. These directions are usually chosen to be symmetric for any ninety degree rotation of the coordinate system. Mathematically, this approximation assumes that the intensity is a sum of delta functions,

$$I(\mathbf{r}, \mathbf{\Omega}, \varepsilon, t) = \sum_{n=1}^{M} I_n(\mathbf{r}, \varepsilon, t)\delta(\mathbf{\Omega} - \mathbf{\Omega}_n). \tag{8}$$

If we insert this into Eq. 1, we find that we have N different equations, one for each direction (or ordinate) $\mathbf{\Omega}_n$,

$$\frac{1}{c}\frac{\partial I_n}{\partial t} + \mathbf{\Omega}_n \cdot \nabla I_n = -\sigma_t I_n + \frac{\sigma_s}{4\pi}\sum_{m=1}^{M} w_m I_m + \sigma_a B(T_m) + S_n, \tag{9}$$

where w_m is an integration weight. Each direction n is coupled to all the others through the scattering term and the material equation. Eq. 9 can be differenced in an upwinded manner, leading to a very efficient algorithms.

The discrete ordinates approximation in more than one spatial dimension has a well-known defect called ray effects [16, 18]. Due to the discrete nature of the angular approximation, particles do not reach regions where they otherwise would, sometimes producing large spatial oscillations in the energy density E. There have been some attempts to eliminate ray effects by introducing extra terms into the equations that act like extra scattering [11, 22].

2.3. Spherical Harmonics

In spherical harmonics approximation, the intensity, I, is expanded with a set of orthonormal functions called the spherical harmonic functions,

$$I(\mathbf{r}, \mathbf{\Omega}, \varepsilon, t) = \frac{1}{\sqrt{4\pi}}\sum_{l=0}^{\infty}\sum_{m=-l}^{l} E_l^m(\mathbf{r}, \varepsilon, t)Y_l^m(\mathbf{\Omega}) \tag{10}$$

$$E_l^m(\mathbf{r}, \varepsilon, t) = \sqrt{4\pi}\int_{4\pi} \overline{Y}_l^m(\mathbf{\Omega})I(\mathbf{r}, \mathbf{\Omega}, \varepsilon, t)\ \mathrm{d}\mathbf{\Omega}\,, \tag{11}$$

where E_l^m is the moment of I with respect to the spherical harmonic function Y_l^m. The lowest order spherical harmonic $Y_0^0 = 1/\sqrt{4\pi}$, which implies that $E_0^0 = E$ is the energy density. The P_N approximation arises when it is then assumed that if $l \geq N$, then moments $E_l^m = 0$.

If we multiply Eq. 1 by each $\overline{Y}_l^m$ and integrate over angle, we get a series of equations for the moments of the intensity I. Each moment E_l^m is only coupled to the moments $E_{l'}^{m'}$, where $l' = l \pm 1$ and $m' = m + \{-1, 0, 1\}$, for a total of six other moments. This system of equations can be written in vector form as

$$\frac{1}{c}\frac{\partial \mathbf{E}}{\partial t} + \mathbf{A}_x\frac{\partial \mathbf{E}}{\partial x} + \mathbf{A}_y\frac{\partial \mathbf{E}}{\partial y} + \mathbf{A}_z\frac{\partial \mathbf{E}}{\partial z} = -\sigma_t\mathbf{E} + \mathbf{S}, \tag{12}$$

where $\mathbf{A_i}$'s are the Jacobians with respect to the i^{th} direction describing the details of how the moments are coupled, $\mathbf{E}$ is a vector of the moments E_l^m, and $\mathbf{S}$ is the source vector and contains the scattering and

material emission terms. The Jacobians $\mathbf{A_i}$ are constant in space and share a remarkable property—the eigenvalues of each matrix are identical. Particles travel in waves through the system at a finite number of speeds determined by these eigenvalues.

The spherical harmonics approximation has a defect called wave effects in the time dependent case. In a vacuum, the system of equations (Eq. 12) can be reduced to a wave equation, and it is possible to get negative energy densities $E = E_0^0$. This is clearly unphysical. Not only is this important for vacuum regions, but on short time scales, interactions with the material become unimportant, and the equations again look like they are in a vacuum. Even in time dependent problems without voids, it is possible to get a negative solution for the energy density E. However, the energy density in steady state problems is always nonnegative.

2.4. Monte Carlo

The Boltzmann transport equation (Eq. 1) and approximations based on it solve for the statistical average of energy densities. It treats the radiation as a continuous field; particles do not really exist. Monte Carlo, on the other hand, embraces the particle as its fundamental feature. Individual photons are simulated from birth to death, modifying the material energy as they travel. When a simulated photon is emitted from the material, it slightly decreases the material energy. This photon travels through the model, occasionally interacting with the material through scattering or absorption events. When the photon is absorbed, the material energy is incremented a little bit.

All of the photon's interactions, including its birth, have certain probabilities of occurring that we can estimate. A pseudo random number generator is used in conjunction with these probabilities to calculate when, where, and what kind of event occurred. Once many particles have been simulated, a reasonable average for the energy density can be estimated.

Implicit Monte Carlo, or IMC, is a particular way to handle the time dependence for radiation transport problems. In IMC, as the photons heat or cool the material during the time step, the probability that photons are emitted from the material change. Despite the name of the method, the material properties such as opacity and density are fully explicit; only the emission rate from the material is treated implicitly. At the end of each time step, the photon population is counted, and the material properties incremented [9].

The biggest disadvantage of IMC is that it is both processor time and memory intensive; otherwise, it generally yields very accurate results once enough particles have been simulated. Until a photon dies in an IMC simulation, it remains in memory. For a three dimensional problem, energy dependent calculation, one million particles would use about 45 MB of memory. (This is an absolute minimum and assumes one double precision variable for each of the three position, two angle, and one energy variables. Other information such as the random number generator state, particle time, etc. can increase this number significantly.)

The estimated error in the IMC calculation is

$$\text{Error} = \alpha \frac{1}{\sqrt{N}}, \tag{13}$$

where α is some proportionality constant and N is the number of particles simulated. This equation implies that in order to achieve a factor of 10 decrease in the estimated error, 100 times more particles need

to be simulated. There are many variance reduction techniques that can be used to dramatically reduce the proportionality constant α, but the general scaling of error with the number particles simulated shown in Eq. 13 still applies. While deterministic approximations (diffusion, S_N, P_N) have a uniform error throughout the system, the Monte Carlo simulation has the largest error where there are the fewest particles. It can been argued that this is actually good because Monte Carlo spends its time getting a good answer where it matters, if that is defined as the highest particle density. (This can be a reasonable assumption.) The deterministic approximations get equally good (or bad) results everywhere.

3. A FEW TEST PROBLEMS

The problems in this section are designed to give some insight as to how the various approximation perform relative to each other. Some of the problems are a test of neutral particle transport; they are not coupled to the material energy at all. All of the calculations are single-group in energy.

3.1. A Line Source in Two Dimensions

The most basic of all time dependent problems is a Green's function problem. In two dimensions this is a pulse of particles is emitted from a line source. In a linear system such as ours without the material equation, solutions to all other time dependent problems are just superpositions of solutions of different Green's function problems. Only a vacuum is considered here; there is no coupling with the material. This test problem is designed to show the fundamental differences in each of the approximations. The defects in each of the approximations that are exposed by this problem will also be seen in all of the other test problems considered in later sections.

The energy density can be solved for analytically for most approximations. Solving the transport equation, Eq. 1, for the intensity I, then integrating over angle to get the energy density E yields

$$E^{\text{transport}} = \frac{E^0}{2\pi} \frac{\mathrm{h}(ct-r)}{ct\sqrt{c^2t^2-r^2}}, \tag{14}$$

where E^0 is the strength of the initial radiation pulse along the line and $\mathrm{h}(x)$ is the unit step function. The general P_N solution is

$$E^{P_N} = \frac{E^0}{\pi} \sum_{\lambda_i \geq 0} r_i l_i \left[\frac{\delta(r-\lambda_i t)}{\sqrt{\lambda_i^2 t^2 - r^2}} - \frac{\lambda_i t\, \mathrm{h}(\lambda_i t - r)}{(\lambda_i^2 t^2 - r^2)^{3/2}} \right], \tag{15}$$

Note that there are regions where the solution for E^{P_N} is negative. This is an essential defect of the P_N equations, not a problem with the numerical implementation. The general S_N solution is

$$E^{S_N} = E^0 \sum_i w_i \delta(\|\mathbf{x} - ct\mathbf{\Omega}_i\|), \tag{16}$$

where the sum over i denotes a sum over all angles. In contrast to the transport and P_N solutions, the S_N solution is a function of both x and y instead of a function of r only. This rotational dependence of the discrete ordinates equations is a factor in the problem called ray effects. In the diffusion case, there is no solution as Eq. 7 is not well defined in a vacuum. The flux limited diffusion code that I have access to had difficulties with this problem, so the results are not included.

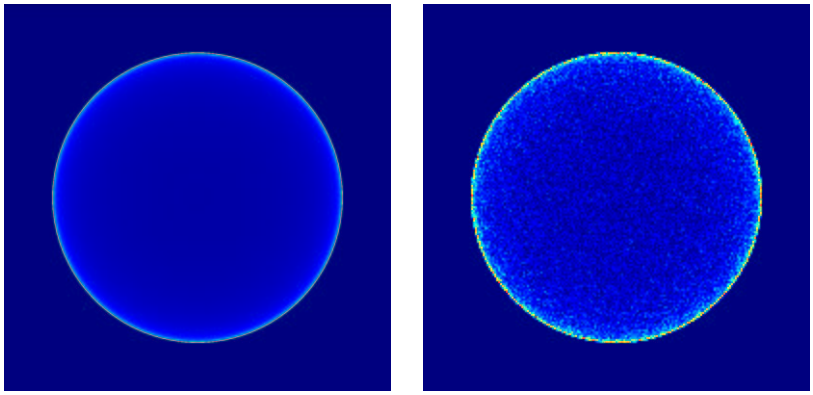

(a) Analytic (b) Monte Carlo

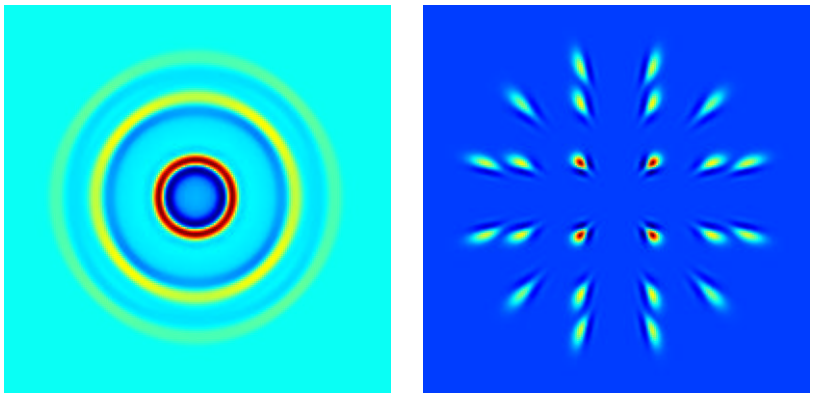

(c) P_5 (d) S_6

Figure 1. Solutions to the pulsed line source problem. The color scale is linear, and the color at each of the corners equals zero for all approximations. Colors more blue than the corners are negative.

Figure 1 shows various numerical solutions for the line source problem. All simulations are on a grid two centimeters square with a mesh spacing of about $dx = 0.01\,\mathrm{cm}$. The Monte Carlo simulation in Figure 1(b) is very similar to the transport solution in Figure 1(a), with the exception statistical noise in the solution. This simulation used one hundred thousand particles. It is fairly easy to reduce this noise by simply increasing the number of particles in the simulation. Figure 1(c) shows that the P_5 solution has three wave speeds. This can be seen in the rings moving away from the center. Just behind each ring, there is a negative region in the energy density. A discrete ordinates S_6 calculation is shown in Figure 1(d). Note that the particles are all moving in delta functions away from the center. Diffusion and flux limited diffusion are not shown because the solutions spread out so fast, they are essentially uniform everywhere.

The full transport equation is hyperbolic in nature, which means that particles and information can only travel at finite speeds. All of the approximations except diffusion respect this; all of the approximation in Figure 1 have semi-reasonable* answers except the diffusion. The key difference between spherical harmonics (P_N) and discrete ordinates (S_N) is that S_N moves particles along particular beams, giving rise to ray-effects; while P_N moves particles only with particular speeds, giving rise to wave-effects. The Monte Carlo simulation looks the best, but if the problem would have been sensitive to instabilities, the

*A "semi-reasonable" answer is one that converges to the correct solution as the order of the method is increased; the results shown in Figures 1(c) and 1(d) are by no means truly reasonable.

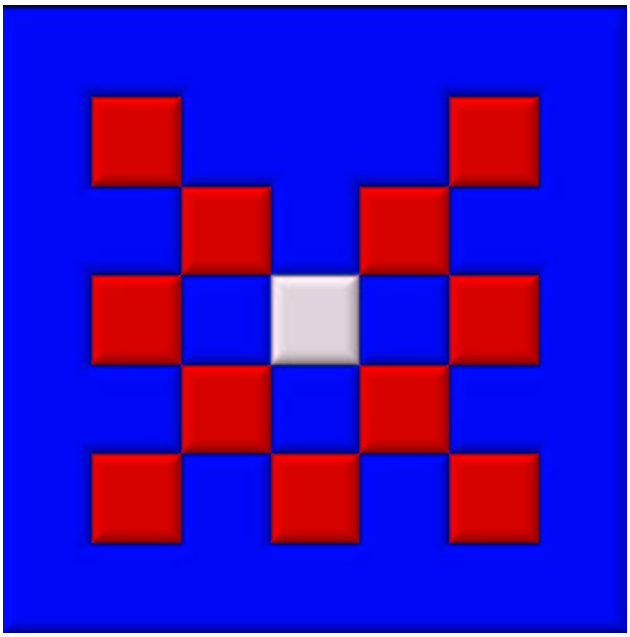

Figure 2. The lattice system. The blue and white regions are pure scattering regions where $\sigma_s = 1\,\mathrm{cm}^{-1}$. Additionally, the white region contains a source of particles. The red regions are pure absorbers with $\sigma_a = 10\,\mathrm{cm}^{-1}$. The particles are simply removed from the system by the absorbers; there is no material equation.

noise in the simulation could be problematic.

3.2. A Lattice Problem

This problem is a checkerboard of highly scattering and highly absorbing regions very loosely based on a small part of a nuclear reactor core. This is only a test of the transport approximations; there is no material energy equation. When an absorption occurs, the particles are simply removed from the system and do not heat it up.

The system for this problem, shown in Figure 2, is seven centimeters wide. The bulk of the lattice is composed of a scattering material with $\sigma_t = \sigma_s = 1\,\mathrm{cm}^{-1}$. There are eleven absorbing regions where $\sigma_t = \sigma_a = 10\,\mathrm{cm}^{-1}$. At time zero, a source of strength one is turned on in the central region of the system. All particles travel at a speed $c = 1\,\mathrm{cm/s}$, and the problem is surrounded on all sides by vacuum boundaries.

Figure 3 shows the energy density E 3.2 seconds after the source is turned on. Results from the diffusion, flux limited diffusion, P_1, P_7, S_6, and implicit Monte Carlo approximations are shown. The diffusion and the discrete ordinates calculations were computed with Sandia's ALEGRA [8]. The implicit Monte Carlo calculation was computed using LLNL's Kull IMC package [10] and used thirty six million particles in half the problem domain, with a reflective boundary on the center line. The P_N calculations were computed with a research code of my own [4, 7].

At the early time shown in Figure 3, particles should have had just enough time to reach the boundaries but

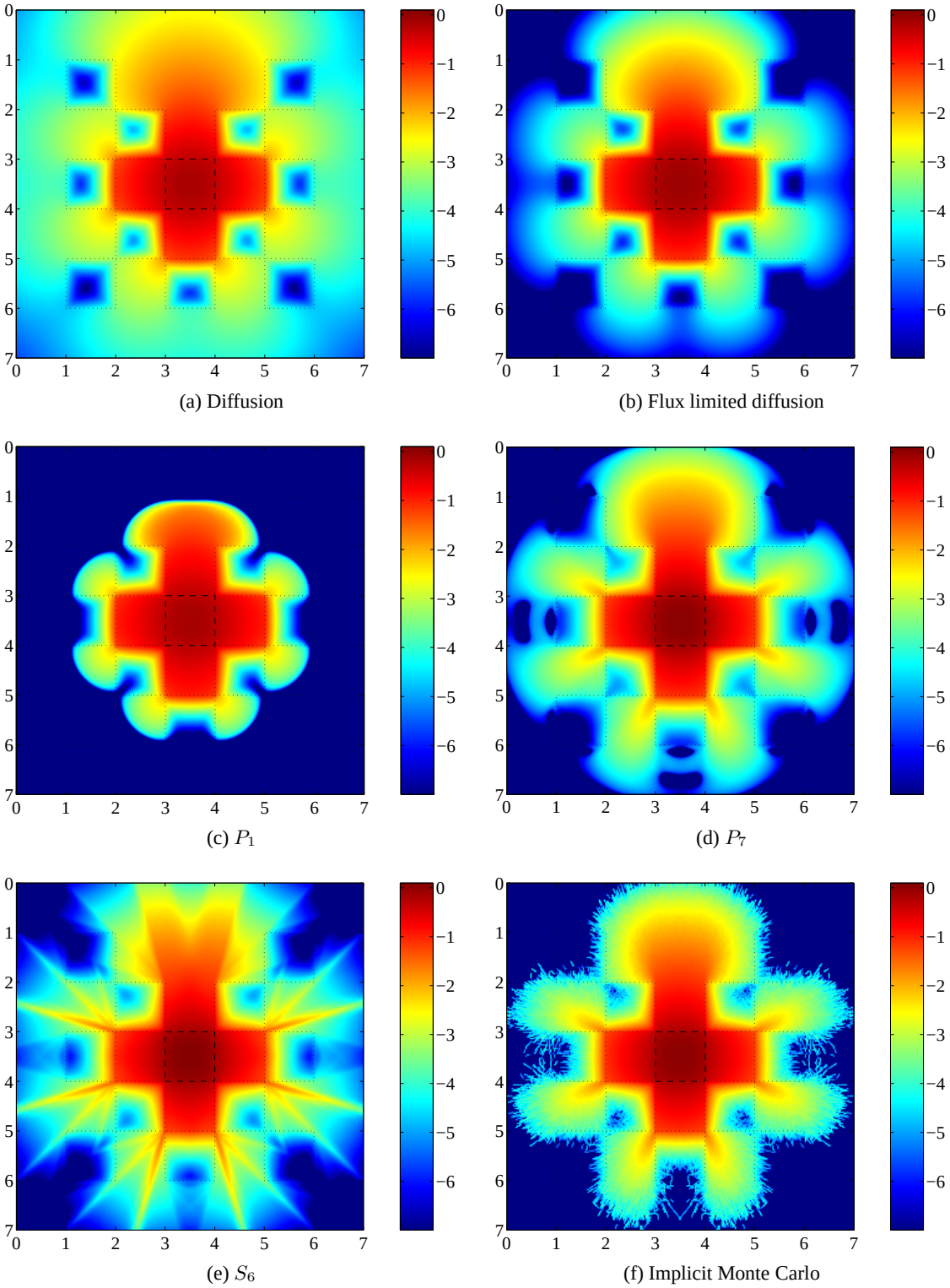

Figure 3. The calculated energy density in the lattice problem 3.2 seconds after the source was turned on. The color-map is proportional to $\log_{10} E$ and limited to seven orders of magnitude.

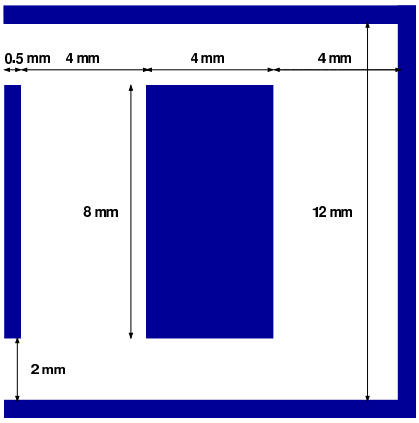

Figure 4. The hohlraum. The blue regions are pure absorbers regions where $\sigma_a = 100\,\mathrm{cm}^{-1}$ and $\rho C_v = 5.0 \times 10^5\,\mathrm{J/m^3\,K}$. The white region is a vacuum.

not enough to reach the corners. The diffusion calculation shown in Figure 3(a) is much too diffuse; the particles have reached all parts of the system. Also, the central region does not have enough particles. The flux limited diffusion result in Figure 3(b) is a vast improvement upon the diffusion calculation and captures the wave front well, but there are no beams of particles leaking between the absorbers as seen in the Monte Carlo and P_7 calculations. The energy density computed using P_1, seen in Figure 3(c), has an artificial wave front of particles traveling at speed $v = 1/\sqrt{3}\,\mathrm{cm/s}$. This is due to the fact that in P_1, the particle waves travel only at this speed. In the P_7 calculation, the particle waves can travel at more speeds, nearly eliminating these nonphysical wave fronts. Some wave-effects can also be seen in the P_7 calculation. Well defined beams of particles leaking between the corners of the absorbing regions in both Figure 3(d) and Figure 3(f), the P_7 and Monte Carlo simulations. Generally P_7 and Monte Carlo agree very well, especially for energy densities above 10^{-4}. The S_6 calculation shown in Figure 3(e) has about the same number of degrees of freedom as the P_7 calculation, but the ray-effects are very dominant.

3.3. A Hohlraum

This hohlraum problem is loosely based on a typical hohlraum for the Z-machine at Sandia. The radiation field is coupled to the the material energy through Eq. 2. Unlike a real hohlraum, this problem is described in Cartesian coordinates. The system, shown in Figure 4, is thirteen millimeters square with a thin wall of material around the outside edge. There are two, two millimeter openings on either left side of the hohlraum, and there is a rectangular block of material in the center of the system. The material is a pure absorber with $\sigma_a = 100\,\mathrm{cm}^{-1}$ and $\rho C_v = 5.0 \times 10^5\,\mathrm{J/m^3\,K}$. The rest of the problem is a vacuum. Some codes used for this problem cannot model a pure void, so the heat capacity is set extremely large, $\rho C_v = 1.0 \times 10^{99}\,\mathrm{J/m^3\,K}$. The opacities are all set to zero in the void. The initial material and radiation temperatures were set to $T_0 = 300\,\mathrm{K}$. A source boundary condition is applied along the entire left hand side. The source temperature is $T_{\text{source}} = 3.5 \times 10^6\,\mathrm{K}$.

Figures 5 and 6 show the radiation temperature at times of $t_1 = 3.93606 \times 10^{-11}\,\mathrm{s}$, and $t_2 = 5.0 \times 10^{-10}\,\mathrm{s}$. The material temperature at $t_2 = 5.0 \times 10^{-10}\,\mathrm{s}$ is shown in Figure 7. Throughout the discussion below, it is assumed that the Implicit Monte Carlo simulation is the most qualitatively correct result.

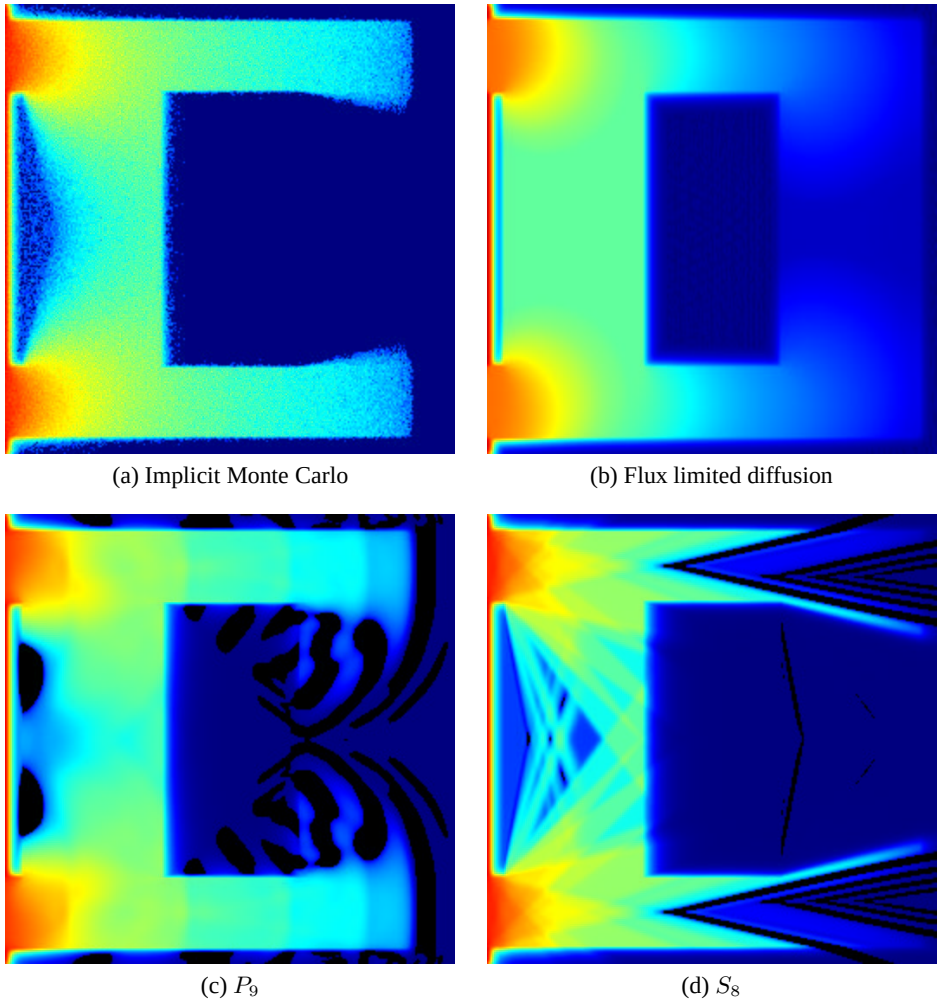

(a) Implicit Monte Carlo (b) Flux limited diffusion

(c) P_9 (d) S_8

Figure 5. The radiation temperature in the hohlraum problem at $t = 3.93606 \times 10^{-11}$ s after the source was turned on. The color-map is proportional to $T_r = (E/a)^{1/4}$. Black regions indicate negative energy densities.

At the time depicted in Figure 5, photons have had nearly enough time to reach the back wall of the hohlraum. Most of the photons are still streaming from the openings; the walls of the hohlraum have not started to heat up yet. Flux limited diffusion, Figure 5(b) has incorrectly allowed photons to fill the entire system. In the P_9, Figure 5(c), simulation, a wave-like solution can be seen, which allow the photons to bend around the front wall and capsule. Notice the black regions in the P_9 solution in Figure 5(c); these represent negative solutions. While too many photons are transported in the wave front around the back side of the wall, P_9 "tries" to compensate by having waves of negative energy follow the positive waves that should not be there. The S_8 is suffering badly from ray-effects. While these ray-effects persist even at long times, the wave effects seen in P_9 solution, Figure 5(c), quickly travel to the right side of the system and are not important at long times.

Finally in Figure 6, the simulation is approaching steady state. Flux limited diffusion, Figure 6(b), has transported too much energy through the problem. In the IMC calculation, Figure 6(a), the back wall is just

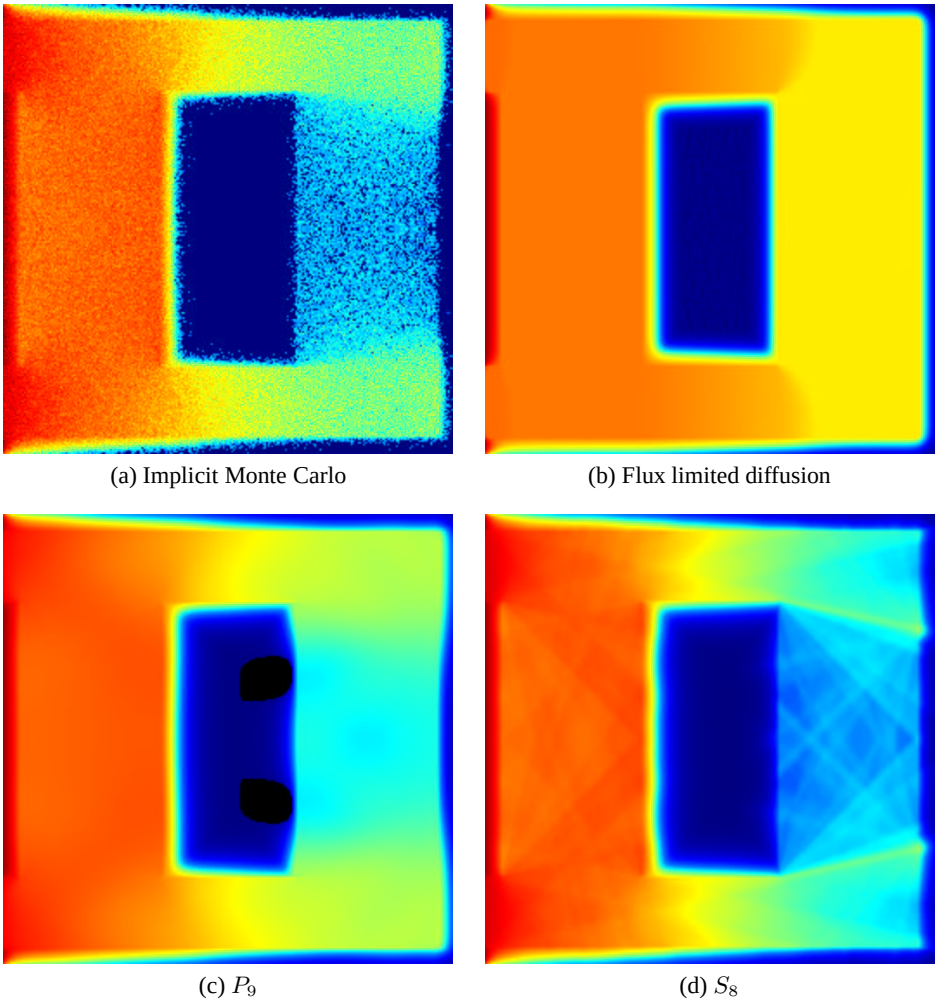

(a) Implicit Monte Carlo (b) Flux limited diffusion

(c) P_9 (d) S_8

Figure 6. The radiation temperature in the hohlraum problem at $t = 5.0 \times 10^{-10}\,\mathrm{s}$ after the source was turned on. The color-map is proportional to $T_r = (E/a)^{1/4}$. Black regions indicate negative energy densities.

starting to heat up and re-emit photons. While the P_9 and S_8 simulations are beginning to qualitatively look good, they still are suffering from wave-effects, Figure 6(c), and ray-effects, Figure 6(d). In the P_9 simulation, the photon energy density has bled around the corners too much.

The material temperature at the final time of $t = 5.0 \times 10^{-10}\,\mathrm{s}$ is shown in Figure 7. Even thought the photon energy density of the IMC is noisy, the calculated material temperature in Figure 7(a) is much smoother. This is because the individual photons of the simulation have a small effect on the material temperature. It takes many photons to change the temperature by a significant amount. This essentially adds an extra level of averaging in the simulation that dramatically improves the quality of the material temperature over what might be expected from the radiation field. Notice that the back side of the capsule has a very uniform temperature; the other higher order methods (S_8 and P_9) are both nonuniform. This could cause problems in instability studies, although the IMC simulation still has some noise, it is just at a much shorter wavelength and smaller amplitude.

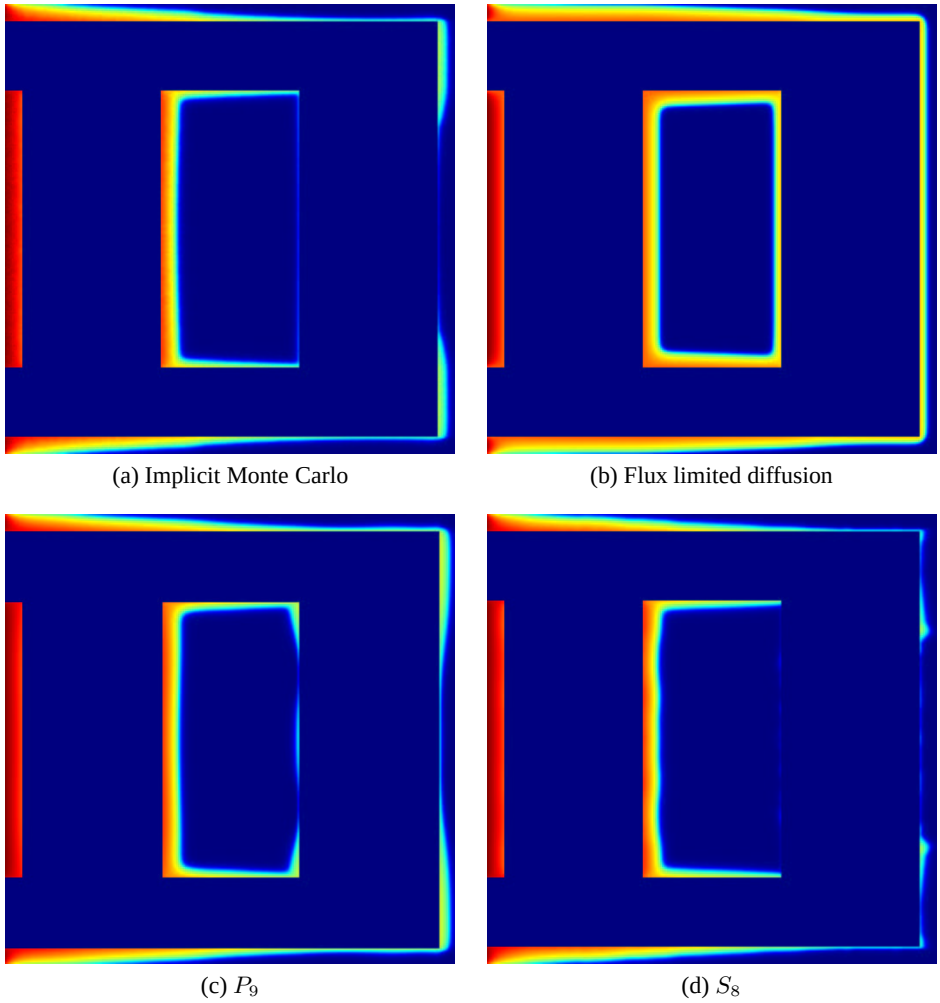

(a) Implicit Monte Carlo (b) Flux limited diffusion

(c) P_9 (d) S_8

Figure 7. The material temperature in the hohlraum problem at $t = 5.0 \times 10^{-10}\,\mathrm{s}$ after the source was turned on. The color-map is proportional to T_m.

4. CONCLUSIONS

Simulating radiation transport is difficult; the equation we would really like to use, the Boltzmann transport equation, is difficult to solve directly. This leads to a myriad of different approximations to the transport equation.

Diffusion is by far the simplest approximation and works well when there is material though which the the photons can diffuse. The many varieties of flux limited diffusion all attempt to improve upon regular diffusion while remaining fairly easy to solve. The errors with diffusion theory all stem from the fact that the fundamental mathematical characteristic of the transport has been changed from hyperbolic to parabolic. This change means that photons are no longer constrained to travel at the speed of light. Some extremely efficient and robust numerical methods have been developed to numerically solve the diffusion theory equations.

The spherical harmonics approximation takes moments of the Boltzmann equation to arrive at a set of conservation laws for each of the moments. In a vacuum, this approximation leads to the wave equations, and this causes the simulations to suffer from wave-effects. Theoretically these effects become negligible when enough moments are used, but in a vacuum, an infinite number of moments are needed to eliminate the wave-effects.

The discrete ordinates approximation moves photons only along a particular set of directions. Many people have studied this approximation, making its problems well understood. Many very efficient algorithms have been developed to solve the discrete ordinates equations. Unfortunately, ray-effects, the most well-known defect of discrete ordinates, can be seen in many simulations.

Implicit Monte Carlo can treat photons exactly, but a given simulation can only simulate a limited number of particles. This leads to statistical noise, which is this method's largest weakness. In order to reduce the amount of noise in a given simulation by a factor of ten, one hundred times more particles must be simulated. In time-dependent problems, not only does this increase run-time by a factor of one hundred, but memory usage also increases by the same factor. The resulting material energy calculated in an IMC simulation, however, is much less noisy than the radiation field, and it is usually the material energy that is more important for simulations.

For the test problems in this paper, the Monte Carlo generally gave the best results. Flux limited diffusion gave the best results normalized by run time. Spherical harmonics and discrete ordinates both have some significant problems in optically thin materials, but spherical harmonics appears to perform better than S_n in highly heterogeneous material such as the lattice problem.

4.1 A Note About Run Times

Several different codes were used to calculate the results. The diffusion and S_n code, is a very general, multipurpose production code. The P_n code is highly tuned and a single purpose code. Because of the large differences in the design of the codes, run time comparisons are very difficult to make fairly.

ACKNOWLEDGMENTS

Sandia is a multiprogram laboratory operated by Sandia Corporation, a Lockheed Martin Company, for the United States Department of Energy under Contract DE-AC04-94AL85000.

REFERENCES

[1] G. I. Bell, S. Glasstone, *Nuclear Reactor Theory*, Krieger (1970).

[2] P. N. Brown, B. Chang, F. Graziani, C. S. Woodward, "Implicit Solution of Large-Scale Radiation-Material Energy Transfer Problems", *Iterative Methods in Scientific Computation II*, pp. 1–14 (1999).

[3] P. N. Brown, U. R. Hanebutte, "Spherical Harmonics Solutions to the 3D Kobayashi Benchmark Suite", in *PHYSOR 2000, ANS International Topical Meeting on the Advances in Reactor Physics and Mathematics and Computation into the Next Millennium*, American Nuclear Society (2000).

[4] T. A. Brunner, *Riemann Solvers for Time-Dependent Transport Based on the Maximum Entropy and Spherical Harmonics Closures*, Ph.D. thesis, University of Michigan (2000).

[5] T. A. Brunner, J. P. Holloway, "Two New Boundary Conditions for Use with the Maximum Entropy Closure and an Approximate Riemann Solver", in *PHYSOR 2000, ANS International Topical Meeting on the Advances in Reactor Physics and Mathematics and Computation into the Next Millennium*, American Nuclear Society (2000).

[6] T. A. Brunner, J. P. Holloway, "One-Dimensional Riemann Solvers and the Maximum Entropy Closure", *Journal of Quantitative Spectroscopy and Radiative Transfer*, **vol. 69**, pp. 543–566 (2001).

[7] T. A. Brunner, J. P. Holloway, "Two Dimensional Time Dependent Riemann Solvers for Neutron Transport", in *M&C 2001 Salt Lake City*, American Nuclear Society (2001).

[8] K. G. Budge, "Verification of the Radiation Package in ALEGRA", Tech. Rep. SAND99-0786, Sandia National Laboratory, Albuquerque, NM (1999).

[9] J. A. Fleck, Jr., J. D. Cummings, "An Implicit Monte Carlo Scheme for Calculating Time and Frequency Dependent Nonlinear Radiation Transport", *Journal of Computational Physics*, **vol. 8**, pp. 313–342 (1971).

[10] N. A. Gentile, N. Keen, J. Rathkopf, "The KULL IMC Package", Tech. Rep. UCRL-JC-132743, Lawrence Livermore National Laboratory, Livermore, CA (1998).

[11] J. Jung, H. Chijiwa, K. Kobayashi, H. Nishihara, "Discrete Ordinate Neutron Transport Equation Equivalent to P_L Approximation", *Nuclear Science and Engineering*, **vol. 49**, p. 1 (1972).

[12] D. S. Kershaw, "Flux Limiting Nature's Own Way", Tech. Rep. UCRL-78378, Lawrence Livermore National Laboratory, Livermore, CA (1976).

[13] D. A. Knoll, W. J. Rider, G. L. Olson, "An Efficient Nonlinear Solution Method for Non-equilibrium Radiation Diffusion", *Journal of Quantitative Spectroscopy and Radiative Transfer*, **vol. 63, no. 1**, pp. 15–29 (1999).

[14] R. J. LeVeque, D. Mihalas, E. A. Dorfi, E. Müller, *Computational Methods for Astrophysical Fluid Flow*, Springer (1998).

[15] C. D. Levermore, G. C. Pomraning, "A Flux-Limited Diffusion Theory", *The Astrophysical Journal*, **vol. 248**, pp. 321–334 (1981).

[16] E. E. Lewis, W. F. Miller, Jr., *Computational Methods of Neutron Transport*, American Nuclear Society (1993).

[17] D. Mihalas, B. Weibel-Mihalas, *Foundations of Radiation Hydrodynamics*, Dover (1999).

[18] W. F. Miller, W. H. Reed, "Ray-Effect Mitigation Methods for Two-Dimensional Neutron Transport Theory", *Nuclear Science and Engineering*, **vol. 62**, p. 391 (1977).

[19] G. N. Minerbo, "Maximum Entropy Eddington Factors", *Journal of Quantitative Spectroscopy and Radiative Transfer*, **vol. 20**, p. 541 (1978).

[20] G. L. Olson, L. H. Auer, M. L. Hall, "Diffusion, P1, and Other Approximate Forms of Radiation Transport", *Journal of Quantitative Spectroscopy and Radiative Transfer*, **vol. 64, no. 6**, pp. 619–634 (2000).

[21] G. C. Pomraning, *The Equations of Radiation Hydrodynamics*, Pergamon Press (1973).

[22] W. H. Reed, "Spherical Harmonic Solutions of the Neutron Transport Equation from Discrete Ordinate Codes", *Nuclear Science and Engineering*, **vol. 49**, p. 10 (1972).

[23] B. Su, “Variable Eddington Factors and Flux Limiters in Radiative Transfer”, *Nuclear Science and Engineering*, **vol. 137**, pp. 281–297 (2001).